Journal of the American College of Cardiology Vol. 47, No. 8, 2006

Published by Elsevier Inc.
ISSN 0735-1097/06/$32.00
doi:10.1016/j.jacc.2005.11.070

Fabry's Disease Cardiomyopathy

Echocardiographic Detection of Endomyocardial Glycosphingolipid Compartmentalization

Maurizio Pieroni, MD, PhD,* Cristina Chimenti, MD, PhD,†‡ Francesco De Cobelli, MD,§ Emanuela Morgante, MD,‖ Alessandro Del Maschio, MD,§ Carlo Gaudio, MD,† Matteo Antonio Russo, MD,‖¶ Andrea Frustaci, MD†‡

Milan and Rome, Italy

OBJECTIVES We sought to identify echocardiographic hallmarks of Fabry's disease cardiomyopathy (FC).

BACKGROUND The recognition of FC from other forms of left ventricular hypertrophy (LVH) by noninvasive imaging techniques is not yet available, and diagnosis, mostly in the absence of systemic manifestations, still relies on genetic and invasive studies.

METHODS Forty consecutive patients (mean age 39 ± 15 years, 22 men and 18 women) with an established diagnosis of Fabry's disease were submitted to echocardiographic evaluation. Control population consisted of 40 consecutive patients with hypertrophic cardiomyopathy (HCM), 40 hypertensive patients with echocardiographic evidence of LVH, and 40 age- and gender-matched healthy subjects with no LVH. All HCM patients and FC with LVH and/or cardiac symptoms underwent cardiac catheterization with left ventricular endomyocardial biopsy.

RESULTS Echocardiography showed in 83% of FC patients (95% of FC patients with LVH) a binary appearance of endocardial border absent in all HCM, hypertensive, and healthy subjects. The sensitivity and specificity of this echocardiographic feature in detecting Fabry patients in study population were 94% and 100%, respectively. Comparison of echocardiographic with histologic and ultrastructural findings showed the binary appearance to reflect an endomyocardial glycosphingolipids compartmentalization, consisting of thickened glycolipid-rich endocardium, free glycosphingolipid subendocardial storage, and an inner severely affected myocardial layer with a clear subendocardial-midwall layer gradient of disease severity.

CONCLUSIONS Echocardiographic binary appearance of left ventricular endocardial border, reflecting endomyocardial glycosphingolipids compartmentalization, represents a sensitive and specific diagnostic hallmark of Fabry's disease cardiomyopathy. (J Am Coll Cardiol 2006;47: 1663–71) © 2006 by the American College of Cardiology Foundation

Fabry's disease is an X-linked disorder caused by deficiency of lysosomal enzyme alpha-galactosidase A, resulting in progressive intracellular accumulation of glycosphingolipids in different tissues, including skin, kidneys, vascular endothelium, ganglion cells of peripheral nervous system, and heart (1). Cardiac involvement is characterized by progressive left ventricular hypertrophy (LVH) that mimics the morphologic and clinical features of hypertrophic cardiomyopathy (HCM) (2,3). Indeed, Fabry's disease cardiomyopathy (FC) has been reported in up to 6% of men (3) and 12% of women (4) with late-onset HCM. In particular, the heart can be the only organ involved in male patients with specific gene mutations (2) and in female carriers where the nearly normal enzymatic activity and the lack of systemic manifestations make its identification more difficult (5). The recognition of Fabry's disease has recently become more relevant as enzyme replacement (6) and enzyme enhancement (7) therapy have proved effective in reducing glycosphyngolipids accumulation and in clearing existing deposits with improvement of cardiac function.

To identify undiagnosed patients affected by FC, assessment of alpha-galactosidase A activity in peripheral blood lymphocytes in all patients with unexplained LVH has been proposed. However, this approach, considering the low prevalence of Fabry's disease in the general population (1), implies relevant costs and therefore may be limited to tertiary referral centers. In addition, measurement of alpha-galactosidase A activity in peripheral blood may be unreliable in female carriers, who frequently show clinical manifestations of the disease in the presence of normal enzymatic activity (4,8). Moreover, even recently developed imaging techniques (9–12) appear ineffective in distinguishing FC from HCM and thereby focusing the enzymatic activity screening in patients with unexplained LVH.

In the present study, we compared echocardiographic features of patients with FC, HCM, and LVH secondary to hypertension in order to identify non-invasive imaging hallmarks in patients with an established diagnosis of FC.

METHODS

Patient population. From January 1996 to December 2004, we studied 40 consecutive patients (mean age 39 ± 15 years, 22 men and 18 women) from 12 different families

From the *Ospedale Multimedica, Milan, Italy; †Heart and Great Vessels Department "Attilio Reale," "La Sapienza" University, Rome, Italy; ‡National Institute for Infectious Diseases "Lazzaro Spallanzani," Rome, Italy; §Radiology Department, San Raffaele Hospital, Milan, Italy; ‖Pathology Department, "La Sapienza" University, Rome, Italy; and ¶"San Raffaele Pisana" Institute, Rome, Italy.
This study was supported by Telethon Foundation grant GGP05264 (Rome, Italy) and partially supported by a grant from Genzyme Europe.

Manuscript received October 4, 2005; revised manuscript received November 1, 2005, accepted November 22, 2005.

JACC Vol. 47, No. 8, 2006
April 18, 2006:1663–71

Abbreviations and Acronyms

CMR = cardiac magnetic resonance
FC = Fabry's disease cardiomyopathy
HCM = hypertrophic cardiomyopathy
LV = left ventricle/ventricular
LVH = left ventricular hypertrophy

who received a diagnosis of Fabry's disease on the basis of reduced alpha-galactosidase A activity in peripheral blood lymphocytes and/or genetic analysis. Among these, 20 patients (group A) presented LVH with a maximal wall thickness ≥15 mm at echocardiographic evaluation, whereas 20 subjects (group B) showed mild (maximal wall thickness <15 mm) (n = 13) or no (n = 7) LVH. The control population consisted of 40 consecutive patients with HCM, 40 hypertensive patients with echocardiographic evidence of LVH, and 40 age- and gender-matched healthy subjects with no LVH.

As our institution is a tertiary referral center dedicated to the study of heart muscle diseases, all HCM patients, all group A Fabry patients, and group B patients presenting cardiac symptoms were submitted to cardiac catheterization with endomyocardial biopsy to assess the severity of cardiac involvement. In addition, all patients with FC and 30 patients with HCM also underwent cardiac magnetic resonance (CMR) with late gadolinium enhancement study as part of the diagnostic process.

Biochemical studies. Alpha-galactosidase A activity was assessed in white blood cells in all patients. Lymphocytes were isolated by gradient centrifugation (Lymphoprep, Nycomed, Oslo, Norway), washed in phosphate-buffered saline, and homogenized in distilled water. The resulting lymphocyte supernatant was assayed with 4-methylumbelliferyl-alpha-D-galactoside for alpha-galactosidase A activity (measured as nanomoles per hour per milligram of protein) (7). Normal values were considered between 1,619 and 3,044 nmol/h/1 mg protein.

Genetic analysis. Genomic deoxyribonucleic acid was isolated from peripheral blood (Puregene DNA isolation kit, Gentra Systems, Minneapolis, Minnesota), and all of the alpha-galactosidase A coding regions and adjacent intronic regions were sequenced as previously described (7).

Echocardiographic studies. All echocardiographic studies were performed with Agilent Sonos 5500 (Hewlett-Packard, Palo Alto, California), Toshiba Powervision 6000 (Toshiba America Medical Systems, New York, New York), and Aplio 80 ultrasound systems (Toshiba America Medical Systems). Patients were imaged, and data were analyzed offline by two experienced investigators unaware of the underlying cardiomyopathy and blind to clinical data. In case of difference in terms of measurement or functional and morphologic assessment, a consensus value was reached in all cases with the help of a third experienced echocardiographer. Left ventricular septal, posterior, and maximal wall thicknesses; end-diastolic and end-systolic dimensions; ejection fraction; fractional shortening; and left atrial volumes were determined according to established criteria (13). Maximal wall thickness was defined as the greatest thickness measured at any segment of left ventricular (LV) wall. A LV outflow gradient >30 mm Hg at rest was considered significant. Peak early (E) and late (A) transmitral filling velocities, E/A ratio, deceleration time of E velocity, and isovolumic relaxation time were measured from mitral inflow velocities (9). In all patients, tissue Doppler studies were also performed as previously described (9).

CMR studies. Cardiac magnetic resonance was performed on a 1.5-T whole-body scanner (Gyroscan Intera Master 1.5 MR System, release 9.0, Philips Medical Systems, Best, the Netherlands) by using an enhanced gradient system with a maximum gradient strength of 30 mT/m and a maximum gradient slew rate of 150 $mT/m^{-1} \cdot s^{-1}$ and a five-element cardiac phased-array coil (SENSE-cardiac). Black blood morphologic images in the cardiac short-axis, four chamber long-axis, and two chamber long-axis planes were acquired by using T2-weighted sequences without and with fat suppression. In the same planes, cine-magnetic resonance imaging was performed by using a breath-hold balanced fast field-echo sequence. The cine-magnetic resonance short-axis images encompassed the entire left ventricle from the base to the apex (stack of 8 to 12 contiguous short-axis slices; thickness = 8 mm, gap = 2 mm) in order to obtain a volumetric evaluation in a three-dimensional fashion. Late enhancement assessment was performed 10 to 15 min after injection of gadolinium-DTPA (Shering AG) (0.2 mmol/kg of body weight), by using a three-dimensional inversion recovery T1-weighted sequence. Two consecutive stacks, each composed of 10 contiguous slices (20 slices; thickness = 5 mm, gap = 0 mm) were acquired in the short-axis plane to encompass the entire left ventricle. Total acquisition time was about 40 min.

CMR imaging analysis. Image analysis was performed using an image-processing workstation (EasyVision, Philips Medical Systems) with the cardiac analysis software package (release 5x). End-diastolic volume, end-systolic volume, stroke volume, and ejection fraction of the LV were calculated. Left ventricle myocardial mass was automatically obtained by multiplying the wall volume with the specific myocardial weight (1.05 g/cm^3). The volume of hyperenhanced tissue was calculated on short-axis images and the percentage of late enhancement was given by the ratio between volume of hyperenhanced tissue and volume of LV myocardium ×100.

The cine and contrast-enhanced images were evaluated separately by the consensus of two expert observers, who assessed the location of any hyperenhanced regions; the enhancement patterns were described as focal, diffuse, or in striae, and wall location was described as subendocardial, mesocardial (midwall), subepicardial, or transmural.

Cardiac catheterization and endomyocardial biopsy. All invasive studies conformed to the Declaration of Helsinki and were performed after patient written informed consent

Table 1. Causal Mutations in the Alpha-Gal Gene Identified in the 12 Fabry Families Studied

Family	Exon/Intron Location	Nucleotide Change	Effect on Coding Sequence	Genotype	Reference
I	Exon 6	C946 delG	Frameshift/stop codon	c946 del G	Morrone 2002
II	Exon 2	c334 C>T	Amino acid change	R112C	Ishii 1992
III	Exon 7	c1133G>A	Amino acid change	C378Y	Topaloglu 1999
IV	Intron3	IVS3 + 1G>A	Splicing defect	IVS3 + 1G>A	Aston-Prolla 2000
V	Exon 1	c119 C>T	Amino acid change	P40L	Aston-Prolla 2000
VI	Exon 6	c982 G>A	Amino acid change	G328R	Ishii 1992
VII	Exon 7	del CT	Frameshift/stop codon	L344-X_{28}-Stop	Germain 1996
VIII	Exon 5	c680A>T	Amino acid change	R227Q	Eng 1993
IX	Exon 1	c126-127 insCATG	Frameshift/stop codon	c126-127 insCATG	Morrone 2002
X	Exon 5	c215 A>G	Amino acid change	N215S	Eng 1993
XI	Exon 6	c835 C>A	Amino acid change	Q279K	Dominissini 2004
XII	Exon 5	c220 C>T	Amino acid change	R220X	Meaney 1994

del = deletion; ins = insertion; IVS = intervening sequence.

and approval by the ethical committee of our institution. All patients submitted to cardiac catheterization underwent coronary and LV angiography with LV endomyocardial biopsy. Endomyocardial biopsies were performed in the septal-apical region of the LV. At least six endomyocardial samples were obtained from each patient and were processed for histology, immunohistochemistry, and transmission electron microscopy (9).

Histology, immunohistochemistry, and electron microscopy. Histology and electron microscopy studies were performed by a pathologist blind to imaging and molecular and genetic studies. Three to four specimens were fixed in 10% buffered formalin and embedded in paraffin wax; 5-μm cut sections were stained with hematoxylin and eosin, Miller's elastic van Gieson, and Masson's thrichrome. One to two samples were immediately frozen in optimal cutting temperature compound with isopentane cooled in liquid nitrogen and stained with periodic acid-Schiff and Sudan black in order to assess the presence of glycolipids storage as previously described (4,7). Two myocardial samples were fixed in 2% glutaraldehyde in 0.1-m phosphate buffer (pH = 7.3) and embedded in Epon resin; semithin sections were processed for Azur II staining while ultrathin sections were stained with uranyl acetate and lead hydroxide (4,7,9) for electron microscopy analysis.

Measurements on myocardial tissue sections were performed using a semi-automated system (Lucia G software version 4.82, Nikon, Japan). The degree of myocyte hypertrophy was assessed by means of cellular diameter at nuclear level in transverse sections. Endocardial thickness was measured in all patients. In addition, in Fabry patients intramyocyte vacuoles as percent of total cell area were measured in 20 random high-power fields (×400) in subendocardial and inner myocardial cells in each specimen, and a mean value was calculated for each patient.

Statistical analysis. Normal distribution of explored variables was assessed with Shapiro-Wilk test. Continuous variables are presented as mean ± SD. Categorical variables are presented as proportions or percentages. Comparisons of proportions between groups were performed with chi-square test; in the case of 2 × 2 tables with an expected cell count of <5, Fisher exact test was used. Between-groups comparisons of variables showing normal distribution and homogeneous variance (as assessed by Levene's test) were performed with one-way ANOVA; in the case of between-groups significant differences at one-way ANOVA, a post-hoc analysis was performed with Scheffé test. Between-groups comparisons of variables not showing normal distribution were performed with Kruskal-Wallis test; in the case of overall between-groups significant differences at Kruskal-Wallis test, direct comparisons were performed with Mann-Whitney test. The significance level was set at $p < 0.05$. In the case of multiple comparisons, the alpha level of Mann-Whitney test was divided by the number of multiple comparisons performed.

RESULTS

Causal mutations identified in the 12 families are reported in Table 1. Each group included both male and female patients from at least nine families. Group B patients were younger than group A (28 ± 9 years vs. 51 ± 12 years, $p < 0.01$) and included a similar number of women (10 vs. 8 in group A). Clinical characteristics, signs, and symptoms of cardiac involvement and extra-cardiac manifestations are reported in Tables 2 and 3. Alpha-galactosidase A activity was very low (mean value 65.6 ± 75.3, range 9.2 to 360.43 nmol/h/mg of protein) in all male patients. Heterozygote females showed from intermediate to very low values of alpha-Gal A activity (mean value 797.9 ± 233.2, range 134.1 to 1,082.15 nmol/h/mg of protein), and clinical manifestations ranged from absence of signs and symptoms of the disease to severe systemic involvement. Complex and repetitive ventricular extrasystoles (Lown class III to IVa) were present at Holter monitoring in 10 group A patients and in 11 group B patients. Extra-cardiac manifestations were present in 16 group A Fabry patients and in 17 group B patients. In female patients clinical manifestations and in particular cardiac involvement were more common and more pronounced with increasing age. In five female carri-

Table 2. Genetic, Clinical and Echocardiographic Features of Patients With Fabry Disease and MWT ≥15 mm

Patient	Age/Gender	Family	Enzymatic Activity* (nmol/h/mg of Protein)	Cardiac Manifestations	Extracardiac Manifestations	MWT (mm)	Binary Endocardial Border
1	46/M	I	20.90 ± 1.46	Dyspnea, chest pain, VA	Skin, eyes, ears, kidneys, CNS, AP, H	21	Yes
2	55/F	I	589.10 ± 46.25	Dyspnea	Eyes, ears, AP, H	20	Yes
3	46/M	II	30.56 ± 6.33	Dyspnea, VA	Skin, eyes, ears, kidneys, CNS, AP, H	19.5	Yes
4	33/M	III	103.08 ± 13.51	VA	AP, skin, eyes	18.5	Yes
5	39/M	IV	360.43 ± 16.34	Dyspnea	AP, skin, eyes	17	Yes
6	35/M	V	9.2 ± 0.19	Dyspnea	AP, skin, eyes	18.5	Yes
7	43/M	VI	136.00 ± 21.1	Dyspnea, chest pain, VA	—	20	Yes
8	49/F	VII	1,027.10 ± 56.47	Dyspnea	—	17	Yes
9	52/F	VIII	923.15 ± 73.00	Dyspnea, VA	—	16.5	Yes
10	48/M	IX	70.26 ± 9.55	Dyspnea, VA	Skin, eyes, H	16	Yes
11	60/F	X	378.48 ± 14.56	Dyspnea	Eyes, ears, kidneys	20	Yes
12	70/F	X	831.62 ± 49.36	Dyspnea, chest pain, VA	Eyes, ears	15.5	Yes
13	40/M	X	75.60 ± 19.42	Dyspnea	Skin, eyes, ears, kidneys, CNS	15.5	Yes
14	69/M	X	50.23 ± 5.62	Dyspnea, chest pain, VA	Eyes, ears, kidneys	19	Yes
15	66/F	XI	964.00 ± 21.52	Dyspnea, VA	Eyes, ears, kidneys	16.5	Yes
16	63/M	XI	36.10 ± 1.90	Dyspnea, chest pain, VA	Eyes	18	Yes
17	61/F	XI	722.47 ± 39.11	Dyspnea, VA	Eyes	17.5	Yes
18	59/F	XI	799.42 ± 37.00	Dyspnea	—	18	Yes
19	35/M	XI	15.23 ± 0.78	Dyspnea, chest pain, VA	Skin, eyes, ears, kidneys, CNS	16.5	Yes
20	41/M	XII	23.11 ± 2.62	Dyspnea, chest pain, VA	Skin, eyes, ears, kidneys	17.5	Yes

*Values are the mean (± SD) results of three independent determinations on peripheral blood lymphocytes.
AP = acroparesthesias; CNS = central nervous system; H = hypoidrosis; VA = ventricular arrhythmias (Lown class III to IVa).

ers, cardiac involvement represented the only manifestation of the disease, whereas in two other female patients ocular involvement was the only accompanying manifestation.

At the time of the present study, all patients were receiving enzyme-replacement therapy according to drugs and dosages currently approved in Europe (either agalsidase beta 1 mg/kg of body weight or agalsidase alpha 0.2 mg/kg of body weight) from at least three months (mean 10 ± 6 months, range 3 to 16 months).

Echocardiographic studies. Main echocardiographic findings are reported in Table 4. Differences between observers occurred in <7% of cases and were always <1.5 mm. In

Table 3. Genetic, Enzymatic and Clinical Characteristics of Patients With Fabry Disease and MWT <15 mm

Patient	Age/Gender	Family	Enzymatic Activity* (nmol/h/mg of Protein)	Cardiac Manifestations	Extracardiac Manifestations	MWT (mm)	Binary Endocardial Border
1	17/F	I	134.12 ± 21.68	—	AP, eyes, ears	10	No
2	23/M	I	28.29 ± 6.52	VA	AP, eyes, ears	13	Yes
3	26/M	I	17.05 ± 3.68	VA	AP, eyes, ears, skin	13	Yes
4	14/F	I	722.10 ± 35.12	—		10	No
5	36/F	II	905.15 ± 52.11	VA	—	12.5	Yes
6	42/F	II	1030.15 ± 78.05	VA	—	13	Yes
7	18/M	III	21.30 ± 3.79	VA, dyspnea, chest pain	—	12.5	No
8	19/M	III	27.59 ± 4.10	VA, dyspnea, chest pain	—	13.5	Yes
9	19/F	VII	1082.15 ± 58.65	—	AP, H	10	No
10	22/M	VII	23.79 ± 4.14	—	AP, skin, ears, eyes	14	Yes
11	27/M	VIII	99.00 ± 19.09	VA	AP	12.5	Yes
12	30/M	VIII	70.00 ± 1.95	VA	AP	14	Yes
13	29/M	IX	123.04 ± 40.27	—	AP, skin, ears, eyes	13	Yes
14	30/M	IX	44.20 ± 7.87	—	AP, skin, ears, eyes	13.5	Yes
15	32/F	X	964.12 ± 42.45	—	—	10.5	No
16	33/F	XI	905.24 ± 33.10	—	Eyes	11	No
17	32/M	XI	59.33 ± 2.78	Dyspnea	Eyes, ears	13	Yes
18	34/F	XI	882.29 ± 19.65	Dyspnea, VA	Eyes, ears	13	Yes
19	40/F	XII	654.55 ± 32.26	Dyspnea, VA	Eyes, ears, kidneys	12.5	No
20	44/F	XII	748.45 ± 29.64	Dyspnea, VA	Eyes, ears, kidneys	14.5	Yes

*Values are the mean (± SD) results of three independent determinations on peripheral blood lymphocytes.
Abbreviations as in Table 2.

Table 4. Echocardiographic Data of Study Population

	FC Group A (n = 20)	FC Group B (n = 20)	HCM (n = 40)	Hypertensive Patients (n = 40)	Controls (n = 40)
Age, yrs	51 ± 12*	28 ± 9*	40 ± 6	40 ± 8	41 ± 6
Men/women, n	12/8	10/10	22/18	20/20	20/20
Maximal wall thickness, mm	17.9 ± 1.6*	12.5 ± 1.4†	27.0 ± 5.0*	12.7 ± 2.6†	8.7 ± 1.0
LV outflow tract gradient	0	0	10 (25%)	0	0
LV end-diastolic diameter, mm	45.8 ± 2.2	47.7 ± 3.2	39.1 ± 3.5*	49.0 ± 3.4	47.0 ± 1.8
LV ejection fraction, %	60 ± 5	64 ± 4	67 ± 5‡	57 ± 7	60 ± 3
Fractional shortening, %	41 ± 4	42 ± 4	40 ± 7	42 ± 6	39 ± 6
E/A ratio	1.0 ± 0.3†	1.2 ± 0.4	1.0 ± 0.7†	1.2 ± 0.3	1.4 ± 0.2
Isovolumic relaxation time, ms	108.7 ± 11.6§	76.6 ± 7.8	109.2 ± 17.8§	87.4 ± 3.4†	78.9 ± 8.7
E-wave deceleration time, ms	220.8 ± 31.4‖	177.3 ± 22.4†	210.2 ± 37.7‖	235.7 ± 36.7‖	185.8 ± 31.4
Restrictive filling pattern	0	0	5 (25)*	0	0
Mitral regurgitation	6 (30)†	5 (25)†	14 (35)†	12 (30)†	0
Endocardial binary appearance	20 (100)¶	13 (65)¶	0	0	0

Data are presented as the mean value ± SD or n (%) of patients. *$p < 0.01$ vs. all other groups; †$p < 0.01$ vs. controls; ‡$p < 0.01$ vs. FC Group A, hypertensive patients and controls; §$p < 0.01$ vs. FC Group B, hypertensive patients and controls; ‖$p < 0.01$ vs. FC Group B and controls; ¶$p < 0.01$ vs. HCM, hypertensive patients, and controls. Analysis of variance was applied in the comparison of ejection fraction, Kruskal-Wallis for all other continuous variables. Chi-square test was applied in all comparisons between categorical variables.

FC = Fabry cardiomyopathy; HCM = hypertrophic cardiomyopathy; LV = left ventricular.

group B Fabry patients, LVH (maximal wall thickness ≥11 mm) was observed in 15 cases. Patients with HCM showed higher maximal wall thickness and lower LV end-diastolic diameter in comparison with both FC and hypertensive patients and more frequently presented asymmetric hypertrophy and outflow tract gradient. No differences in terms of ventricular and atrial dimensions, systolic function, or presence and degree of mitral regurgitation were observed between HCM and group A patients. Diastolic function was systematically impaired with a similar prevalence of restrictive filling pattern in HCM and group A patients.

Among subjects with FC, all group A patients and 13 group B patients showed a binary appearance of LV endocardial border, more evident in the left side of interventricular septum but observable in most cases all along the LV chamber contour and, in some patients with marked LVH and an optimal acoustic window, even in the right side of interventricular septum and free right ventricular wall (Fig. 1A). Interestingly, binary endocardial appearance also was observed in three group B patients (Patients #10, #13, and #14 in Table 2) presenting mild LVH but no symptoms of cardiac involvement

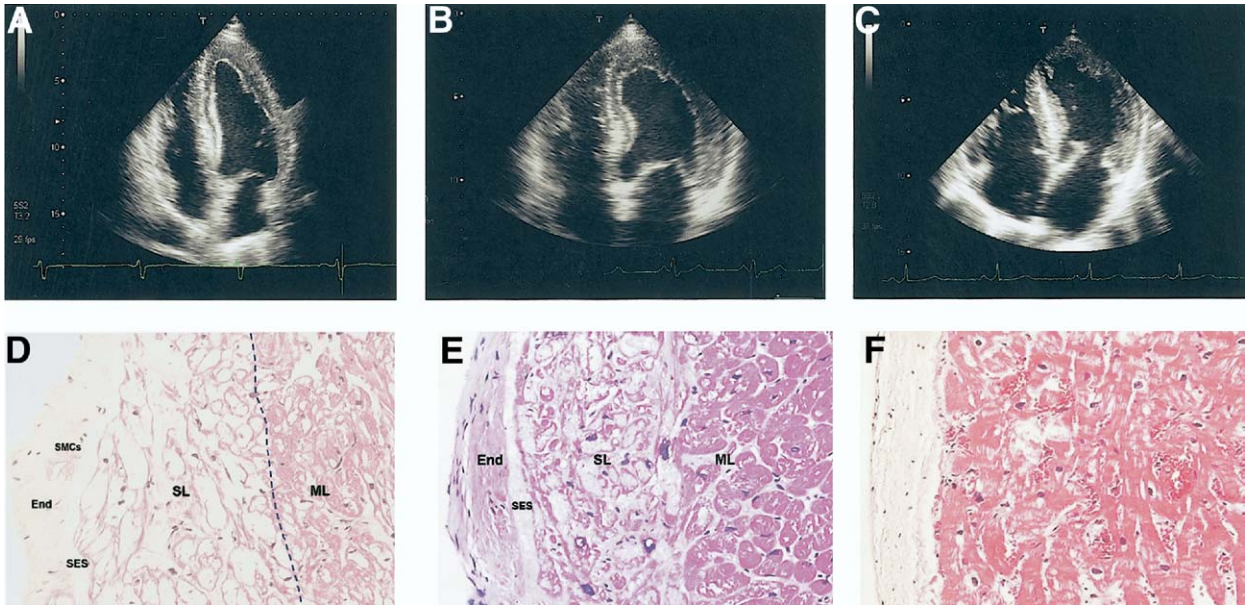

Figure 1. Two-dimensional echocardiography in four-chamber apical view and left ventricular endomyocardial biopsy from two patients (Patient #4 and Patient #18 of Table 2) with Fabry's disease cardiomyopathy (**A,D** and **B,E**, respectively) and a patient with hypertrophic cardiomyopathy **(C,F)**. Comparison of the three echocardiographic frames reveals the presence of a binary appearance of left ventricular endocardial border in the two Fabry patients **(A,B)**. This echocardiographic finding reflects the glycosphingolipids compartmentalization involving a thickened endocardium (End) with enlarged and engulfed smooth muscle cells (SMC), a subendocardial empty space (SES), and a prominent involvement of subendocardial myocardial layer (SL), while the middle layer (ML) appears partially spared **(D,E)**. The echocardiographic pattern is absent in hypertrophic cardiomyopathy **(C)**, despite a similar thickening of the endocardium **(F)**.

Table 5. Tissue Doppler Data of Study Population

	FC Group A (n = 20)	FC Group B (n = 20)	HCM (n = 40)	Hypertensive Patients (n = 40)	Controls (n = 40)
Septal Sa, cm/s	6.4 ± 0.8*	8.3 ± 0.8†	5.9 ± 0.6*	9.3 ± 1.7†	14.12 ± 1.78
Septal Ea, cm/s	6.0 ± 0.9*	8.5 ± 0.6‡	5.6 ± 1.1*	8.7 ± 2.0†	15.01 ± 2.05
Septal Aa, cm/s	6.8 ± 1.0*	8.9 ± 0.3†	6.4 ± 1.4*	9.3 ± 1.9†	10.5 ± 1.9
Septal Ea/Aa, cm/s	0.97 ± 0.2‡	0.98 ± 0.34†	0.96 ± 0.21‡	0.99 ± 0.19†	1.7 ± 0.4
Septal E/Ea, cm/s	13.6 ± 2.0*	9.78 ± 1.32§	13.9 ± 1.1*	9.6 ± 1.4†	6.1 ± 1.0
Lateral Sa, cm/s	6.5 ± 0.8*	8.6 ± 0.8‡	6.2 ± 1.0*	10.1 ± 1.3†	13.2 ± 1.5
Lateral Ea, cm/s	6.2 ± 1.0*	8.9 ± 0.5†	5.8 ± 0.7*	9.6 ± 2.2†	13.1 ± 2.1
Lateral Aa, cm/s	7.4 ± 1.4*	9.1 ± 0.7†	7.1 ± 1.3*	10.1 ± 1.7	10.1 ± 1.6
Lateral Ea/Aa, cm/s	0.96 ± 0.17†	0.99 ± 0.11†	0.91 ± 0.23‡	1.04 ± 0.24†	1.4 ± 0.4
Lateral E/Ea, cm/s	11.95 ± 3.0*	9.3 ± 1.15‡	12.9 ± 2.1*	8.65 ± 2.3†	5.5 ± 1.5

*$p < 0.01$ vs. FC Group B, hypertensive patients and controls; †$p < 0.01$ vs. controls; ‡$p < 0.01$ vs. hypertensive patients and controls. All comparisons were performed by Kruskal-Wallis test.

Abbreviations as in Table 4.

(Fig. 1B). In the Fabry patient population studied, the prevalence of the echocardiographic feature was 82.5%, reaching 94% when considering only patients with LVH. These findings were reported by all echocardiographers who analyzed images and were considered independent from the ultrasound system used, from gain settings, and mostly from the application of tissue harmonic imaging software. Remarkably, this binary appearance of endocardial border was not observed in any of the HCM (Fig. 1C) and hypertensive patients or in healthy control subjects included in the study. In these settings, the sensitivity and specificity of echocardiographic binary appearance in our population of patients with mild to severe LVH were 94% and 100%, respectively, with a positive predictive value of 100% and a negative predictive value of 94%.

Tissue Doppler analysis showed a significant reduction of both diastolic and systolic velocities in all three groups compared with control patients (Table 5). Remarkably, no significant difference was observed between group A patients and HCM patients in terms of myocardial velocities. Interestingly, group B patients were mostly undistinguishable from hypertensive subjects on the basis of echocardiographic and tissue Doppler findings, as only systolic velocity at lateral corner was significantly different in the two groups.

CMR imaging analysis. Cardiac magnetic resonance confirmed the LV morphologic and functional data observed at echocardiography in all patients. No specific signal in the endocardial and subendocardial layers distinguishing FC from HCM was observed. Gadolinium contrast-enhancement studies showed the presence of late enhancement in 20 patients (50%) with HCM and in 10 group A patients (50%) with FC.

In HCM, contrast enhancement showed a focal pattern in 15 cases and a diffuse pattern in 5 cases. Focal late enhancement areas were mostly localized in the interventricular septum and papillary muscles, but in nine patients with concentric hypertrophy, the areas were also localized in the basal segments of lateral and inferior wall. In patients with FC, late enhancement was localized in all cases in the basal or basal-medium segments of lateral and infero-lateral walls as previously reported (10). In one patient with more severe LV hypertrophy (Patient #1 of Table 2), a focal midwall late-enhancement area was also observed at the apex. The mean percentage of myocardium involved by late gadolinium enhancement in FC patients was 7.8 ± 7.4% (range 0 to 19%).

Cardiac catheterization. All HCM patients and 35 Fabry patients, including all group A patients and 15 group B patients, were submitted to cardiac catheterization and endomyocardial biopsy. In the remaining five group B patients, all of them female carriers, cardiac catheterization was not performed, as the patients did not present LVH or cardiac symptoms. In all cases, coronary angiography was normal and all HCM and FC patients showed increased LV end-diastolic pressure with higher values in HCM (23.2 ± 7.3 mm Hg) and group A patients (21.1 ± 6.4 mm Hg) compared with group B patients (15.6 ± 5.8 mm Hg, $p < 0.01$).

Histology, immunohistochemistry, and electron microscopy. In all patients with Fabry's disease, histology showed at hematoxylin and eosin staining a diffuse vacuolization of myocytes, endothelial cells, and smooth muscle cells; these vacuoles were positive at Sudan-Black staining and consisted at electron microscopy of concentric lamellar figures in single-membrane bound vesicles (myelin bodies), denoting glycosphingolipids accumulation. A gradient in myocardial disease severity was observed in all patients; the subendocardial layers were more severely affected in comparison with outer myocardial layers: subendocardial myocytes were bigger (diameter at nuclear level 60 ± 12 μm vs. 28 ± 13 μm in group A, 44 ± 9 μm vs. 19 ± 7, $p < 0.001$ in group B) and characterized by larger intracellular glycolipid vacuoles than midwall layer myocytes (79 ± 12% vs. 31 ± 9% of cell area in group A; 45 ± 15% vs. 22 ± 6% in group B, $p < 0.001$) (Figs. 1D and 1E). As previously described (4), female carriers presented a patchy distribution of affected areas in the outer myocardial layers but a similar gradient of disease severity.

The endocardium was severely thickened (88 ± 12 μm, range 73 to 100 μm in group A; 64 ± 13, range 42 to 79 μm in group B) mostly due to glycolipid-engulfed

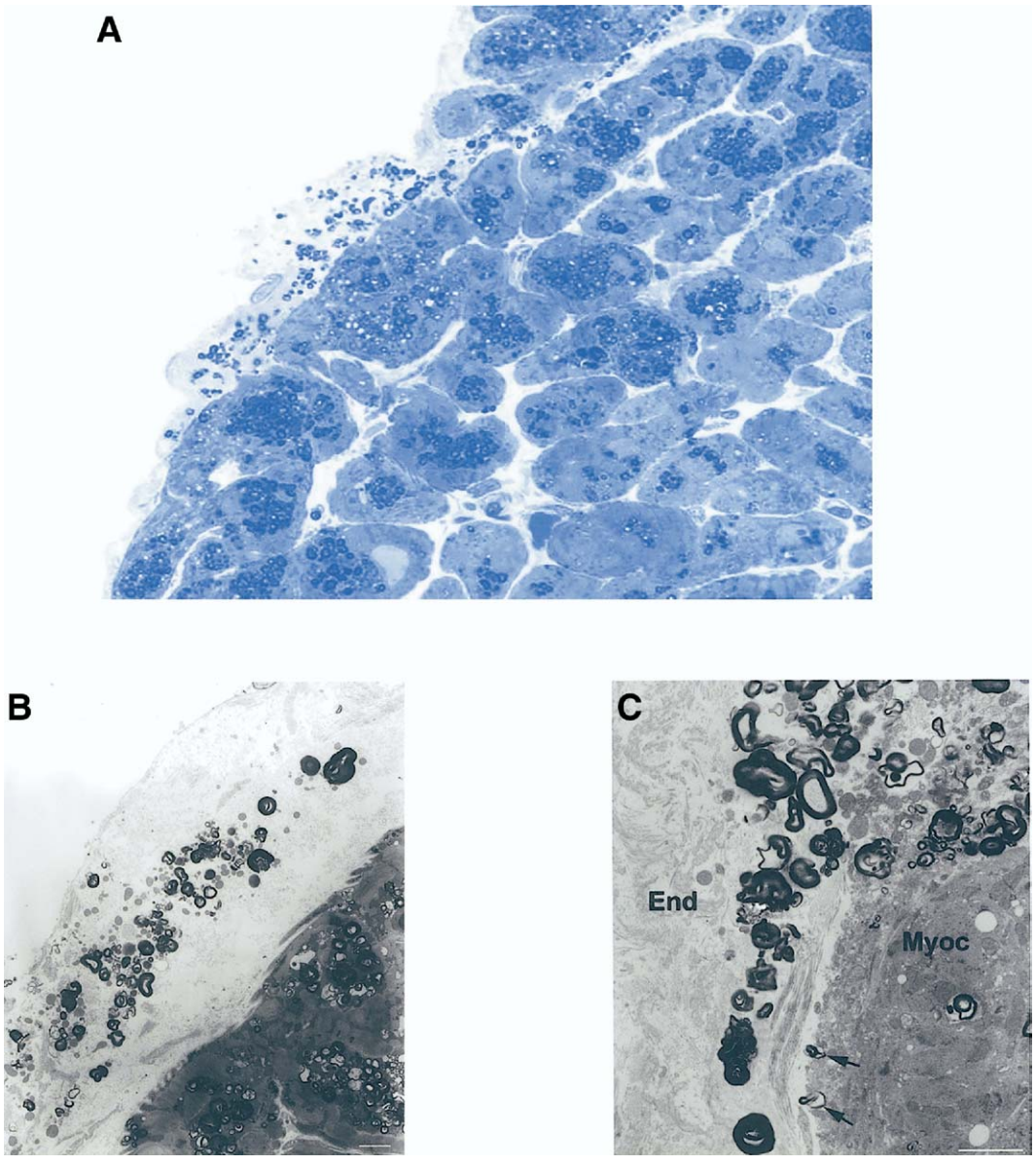

Figure 2. Semithin **(A)** and ultrathin **(B,C)** sections from left ventricular endomyocardial biopsy of the same patient of Figures 1A and 1D. In panel **A,** osmiophilic bodies intensely stained by Azur II are seen in the endocardium, in the subendocardial space, and in myocardium. In the subendocardial space, they are localized in the region of empty spaces seen at H and E histology sections. In the myocardial tissue, a gradient of storage material can be appreciated from the subendocardial to the inner layer. At electron microscopy **(B,C)** the osmiophilic bodies appear to consist of glycosphingolipids organized in membrane-bounded bodies diffusely present in the context of the endocardium (End), occupying the subendocardial space as a free storage material and inside the myocytes (Myo). **Arrows** indicate membrane-bounded bodies at the boundaries between a myocardiocyte and the subendocardial space, suggesting a process of release from the cell to the extracellular space. **(A)** Azur II original magnification ×100. **(B,C)** Bars = 1 μm.

endothelial and smooth muscle cells and free glycosphingolipids. In addition, an empty space between endocardium and myocardium observed at histology (Fig. 2A) appeared to be represented at electron microscopy by free glycosphingolipids organized in myelin bodies (Fig. 2B). The extracellular glycosphingolipids observed in endocardium and subendocardial space were found to derive from death of severely affected cells as well as from glycolipid secretion by massively engulfed cells, as shown at electron microscopy (Fig. 2C). The combination of endocardium, subendocardial empty space, and severely affected myocardium constituted a glycolipid-rich inner layer in all patients, with a mean thickness of 640 ± 118 μm, (range 500 to 800 μm) in group A patients and 440 ± 98 μm (range 290 to 540 μm) in group B.

In HCM patients, histology showed in all cases the presence of severely hypertrophied myocardiocytes, often in total disarray and frequently interrupted in short runs because of interstitial and various degrees of replacement fibrosis. In these patients, the endocardium was significantly thickened (86 ± 32 μm, range 50 to 110 μm) owing to an increase of fibrous tissue (Fig. 1F). At electron microscopy,

myocardiocytes were frequently characterized by sarcomere disorganization.

Correlation between imaging and pathology findings in Fabry patients. With regard to the process of image formation, at ultrasound evaluation fat/muscle interface is characterized by both a significant refraction, with about 19 degrees of deviation (14), and reflection, with percent of energy reflected higher than muscle/blood interface (15). In addition, the glycosphingolipid nature of intracellular storage material organized in concentric lamellar bodies further increases the acoustic impedance of affected tissues (16), leading the digital image processing to depict an echodense and thick endocardial border paralleled by shadowing of the midwall portion of ventricular walls. Concerning the spatial resolution of ultrasound technique, as well as the shrinking of myocardial samples produced by fixation, inclusion, and staining procedures, the previously mentioned inner glycolipid-rich layer may reasonably account for the images observed at two-dimensional echocardiography.

DISCUSSION

Non-invasive identification of cardiomyopathies characterized by LV wall thickening is often difficult, and differential diagnosis frequently relies on invasive studies such as endomyocardial biopsy or molecular and gene analysis. In particular, FC shares several clinical and morphologic features with HCM (4–8), including electrocardiographic and echocardiographic signs of LVH, reduced diastolic and systolic tissue Doppler velocities (9,11), and late-enhancement myocardial areas at cardiac magnetic resonance (10,12). In these settings, in the absence of systemic manifestations of the disease, as observed in the cardiac variant (3,8) and frequently in female carriers (6,7), FC may appear undistinguishable from HCM and other forms of unexplained LVH, as demonstrated by recent studies reporting a significant prevalence of previously unrecognized FC in male and female patients with an established diagnosis of HCM (3,4). Nevertheless, the recent development of specific therapeutic strategies (6,7) may change the natural history and prognosis of FC, making more relevant a proper and early diagnosis.

In the present study, we identified a specific echocardiographic feature of FC reflecting the peculiar pathological substrate of the disease observed at histology and ultrastructural analysis of endomyocardial biopsy tissue. Ultrasound examination in Fabry patients revealed a binary appearance of LV endocardial border, systematically absent in HCM and hypertensive patients as well as in normal control patients, thereby resulting in a distinguished echocardiographic feature with a sensitivity and specificity of 94% and 100%, respectively. The pathological substrate underlying echocardiographic findings was represented by an endocardial and subendocardial glycosphingolipid compartmentalization consisting of close succession of a thickened endocardium, rich in glycolipid-engulfed endothelial and smooth muscle cells, a free glycosphingolipids subendocardial layer, an inner portion of severely affected myocardium, and outer mildly to moderately affected myocardial tissue. This endocardial-epicardial gradient of disease severity observed in our Fabry patients is common in storage and infiltrative cardiomyopathies and has been recently reported in a study comparing CMR and pathology findings in cardiac amyloidosis (17). The possible mechanism underlying this feature may be represented by the remarkable increase of LV end-diastolic pressure, leading to hypoperfusion and prominent damage of subendocardial layers preceding the development of relevant LVH (9).

Concerning the process of image formation, and when considering the spatial resolution limits of the imaging techniques, this complex pathological substrate can be regarded as an inner glycolipid-rich layer including endocardium, free glycosphingolipids, and severely affected myocardium, and an outer layer represented by a mildly affected myocardium corresponding to the midwall portion of ventricular wall. In these settings, ultrasounds depict a thick hyper-echogenic layer representing the inner glycolipid-rich layer, paralleled all along the ventricular contour by an hypo-echogenic layer reflecting the mildly affected midwall myocardium, or possibly a shadowing artifact explained by the high reflection and refraction index of the intracellular lipids-rich layers. On this basis, whether a realistic reproduction of the pathological substrate or a combination of true images with artifacts, the identification of a disease-specific glycosphingolipids subendocardial compartmentalization strongly supports the reliability of binary endocardial appearance as a non-invasive hallmark of FC. Interestingly, CMR gadolinium-enhancement studies failed to identify any endocardial abnormalities in our Fabry patients, whereas myocardial areas of late enhancement in the postero-basal segment previously described as typical of FC (10) were present in 10 out of 20 Group A patients. These findings are not surprising, as late gadolinium-enhancement mostly reflects interstitial expansion even in endocardial and subendocardial portions of ventricular wall, as recently reported by Maceira et al. in cardiac amyloidosis (17) and therefore could not identify the prevalent intracellular glycolipid accumulation occurring in subendocardial layers of FC.

Clinical implications. The echocardiographic detection of endomyocardial compartmentalization was observed in 94% of patients with FC and LVH and was not detectable in five patients with no LVH and in two patients with initial LV wall thickening. These findings confirm that binary endocardial pattern reflects the progressive deposition of glycosphingolipids and, therefore, the severity of the cardiac involvement. The presence of binary aspect of the endocardium even in younger patients with mild LVH strengthens its diagnostic value, supporting its clinical utility in extensive screening and probably in monitoring treatment efficacy.

With this regard, it must be emphasized that the diagnosis of Fabry disease relies mostly on clinical evaluation,

including the assessment of systemic manifestations as well as the evaluation of family members; nevertheless, these issues may result unattended in the absence of remarkable extra-cardiac signs, as frequently occurring in the cardiac variant of the disease and mostly in female carriers. In clinical practice, given that the heart and the kidney are the organs more frequently affected, the screening of HCM and dialysis patients through the assessment of alpha-galactosidase A activity in peripheral blood has been proposed to identify undiagnosed Fabry patients. Nevertheless, this approach, possibly useful in the identification of affected men despite a significant number of false positives (18), provides unreliable results in the screening of female carriers (8). In addition, the screening of large populations may be expensive and therefore available only in referral centers. On the contrary, the non-invasive hallmark we recognized, characterized by high specificity and sensitivity, appears easy to detect in any echocardiography lab and may therefore be considered as a first filter to focus the enzymatic and genetic tests in a more selected population.

Conclusions. Binary appearance of LV endocardial border, reflecting the endocardial and subendocardial compartmentalization of glycosphingolipid material, can be recognized at two-dimensional echocardiography in patients with FC. These findings provide a specific and sensitive non-invasive tool to distinguish FC from other forms of LV hypertrophy promptly allowing its specific treatment.

Reprint requests and correspondence: Dr. Andrea Frustaci, The Heart and Great Vessels Department "Attilio Reale," La Sapienza University, viale del Policlinico 155, 00100 Rome, Italy. E-mail: biocard@rm.unicatt.it.

REFERENCES

1. Desnick RJ, Ioannou YA, Eng CM. α-Galactosidase A deficiency: Fabry disease. In: Scriver CR, Beaudet AL, Sly WS, et al., editors. The Metabolic and Molecular Bases of Inherited Disease. New York, NY: McGraw-Hill, 2001:3733–74.
2. Nakao S, Takenaka T, Maeda M, et al. An atypical variant of Fabry's disease in men with left ventricular hypertrophy. N Engl J Med 1995;333:288–93.
3. Sachdev B, Takenaka T, Teraguchi H, et al. Prevalence of Anderson-Fabry disease in male patients with late onset hypertrophic cardiomyopathy. Circulation 2002;105:1407–11.
4. Chimenti C, Pieroni M, Morgante E, et al. Prevalence of Fabry disease in female patients with late-onset hypertrophic cardiomyopathy. Circulation 2004;110:1047–53.
5. Whybra C, Kampmann C, Willers I, et al. Anderson-Fabry disease: clinical manifestations of disease in female heterozygotes. J Inherit Metab Dis 2001;24:715–24.
6. Eng CM, Guffon N, Wilcox WR, et al. Safety and efficacy of recombinant human alpha-galactosidase A replacement therapy in Fabry's disease. N Engl J Med 2001;345:9–16.
7. Frustaci A, Chimenti C, Ricci R et al. Improvement in cardiac function in the cardiac variant of Fabry's disease with galactose-infusion therapy. N Engl J Med 2001;345:25–32.
8. Linthorst GE, Vedder AC, Aerts JM, Hollak CE. Screening for Fabry disease using whole blood spots fails to identify one-third of female carriers. Clin Chim Acta 2005;353:201–3.
9. Pieroni M, Chimenti C, Ricci R, et al. Early detection of Fabry cardiomyopathy by tissue Doppler imaging. Circulation 2003;107: 1978–84.
10. Moon JC, Sachdev B, Elkington AG, et al. Gadolinium enhanced cardiovascular magnetic resonance in Anderson-Fabry disease. Evidence for a disease specific abnormality of the myocardial interstitium. Eur Heart J 2003;24:2151–5.
11. Nagueh SF, Bachinski LL, Meyer D, et al. Tissue Doppler imaging consistently detects myocardial abnormalities in patients with hypertrophic cardiomyopathy and provides a novel means for an early diagnosis before and independently of hypertrophy. Circulation 2001; 104:128–30.
12. Moon JC, McKenna WJ, McCrohon JA, Elliott PM, Smith GC, Pennell DJ. Toward clinical risk assessment in hypertrophic cardiomyopathy with gadolinium cardiovascular magnetic resonance. J Am Coll Cardiol 2003;41:1561–7.
13. Schiller NB, Shah PM, Crawford M, et al. Recommendations for quantitation of the left ventricle by two-dimensional echocardiography: American Society of Echocardiography Committee on Standards, Subcommittee on Quantitation of Two-Dimensional Echocardiograms. J Am Soc Echocardiogr 1989;2:358–67.
14. Allen MN. Echocardiography. 2nd edition. Philadelphia, PA: Lippincott Williams & Wilkins, 1999.
15. Feigenbaum H, Armstrong WF, Ryan T. Echocardiography. 6th edition. Philadelphia, PA: Lippincott Williams & Wilkins, 2004.
16. Glass RB, Astrin KH, Norton KI, et al. Fabry disease: renal sonographic and magnetic resonance imaging findings in affected males and carrier females with the classic and cardiac variant phenotypes. J Comput Assist Tomogr 2004;28:158–68.
17. Maceira AM, Joshi J, Prasad SK, et al. Cardiovascular magnetic resonance in cardiac amyloidosis. Circulation 2005;111:186–93.
18. Kotanko P, Kramar R, Devrnja D, et al. Results of a nationwide screening for Anderson-Fabry disease among dialysis patients. J Am Soc Nephrol 2004;15:1323–9.